SELF-SENSING TOOL HOLDER FOR IN-PROCESS METROLOGY OF CUTTING FORCE IN ULTRA-HIGH-PRECISION SINGLE-POINT DIAMOND TURNING APPLICATIONS

PETER BABATUNDE ODEDEYI, KHALED ABOU-EL-HOSSEIN, SHAHROKH HATEFI & FUNSHO OYEKUNLE
Precision Engineering Laboratory, Department of Mechatronics, Nelson Mandela University, South Africa.

ABSTRACT
In turning processes, cutting force is of great importance since many cutting force features are useful for predicting and detecting tool conditions. To precisely measure cutting forces, many commercial devices have been developed; however, they are costly, cumbersome, and some implementation restrictions could hinder their suitability in real applications. In this work, a simple, portable, and low-cost tool holder sensor was designed and developed to sense strain and measure cutting force applied during ultra-precision diamond turning. The device can assess cutting intensity up to 3 N with a high sensitivity of 4.592 mV/N or 0.004592 V/N, a calibration test variability of 99.6%, and a percentage error of 2.19, according to static calibration testing.
Keywords: cutting force, force sensor, in-process metrology, single-point diamond turning, strain gauge.

1 INTRODUCTION

In advanced manufacturing technologies, one of the important machining parameters is cutting force [1]. The cutting forces in high-precision metal cutting are directly related to the machining conditions and process parameters. When examining the cutting behavior of difficult-to-machine materials, cutting force is especially relevant [2, 3]. The cutting forces could negatively affect the generation of friction, the consistency of the machined surface, and the dimensional accuracy of the workpiece. It has shown that reducing the cutting forces can improve the tool life and decrease the tool wear [4, 5]. The measurement of cutting forces is often used as an indicator in the design of a machine tool and to optimize the cutting mechanisms [6, 7].

Yet metrology solutions in advanced manufacturing technologies, for in- process measurement of cutting parameters during machining, have recently been emerging. The commercial sensors have low precision, resolution, and repeatability, therefore, not suitable to be used as a metrology solution in advanced manufacturing methods. Recently, by using different sensor integration techniques, metrology solutions have been developed for in-process measurement of cutting forces during different advanced manufacturing methods [8–13].

Byrne *et al.* [14], developed an integrated force sensor solution for drilling operations by integrating two piezoelectric force sensing rings into a direct-driven motor spindle. In another study [15], a force ring was incorporated into the spindle housing for measuring the triaxial cutting force [1]. Totis *et al.* [16] developed a rotating dynamometer for the milling process by installing commercial piezoelectric triaxial force sensors between the modular cartridge and the cutter body. Also, a range of integrated sensor techniques have been developed for the measurement of the feed and transverse forces, as well as torque, during

© 2022 WIT Press, www.witpress.com
ISSN: 2046-0546 (paper format), ISSN: 2046-0554 (online), http://www.witpress.com/journals
DOI: 10.2495/CMEM-V10-N4-329-344

the milling process [17, 18]. In another solution, a piezoelectric thin film polyvinylidene fluoride strain sensor was mounted on the cutting tool shank during the milling process, and all the electronics and batteries were mechanically connected to the tool holder in a metal housing [1]. Albrecht *et al.* [19] designed a system of measuring only the radial cutting force by integrating capacitive sensors into the spindle in order to measure the static and dynamic variation of the distance between the sensor head and the rotating spindle shaft [1]. Different types of commercial piezoelectric rotating dynamometers, such as Kistler Instrument Corporation, have been manufactured [20], and some of these devices can simultaneously recognize four-component cutting forces with good dynamic performance. Yet, these products are expensive.

Rizal *et al.* [6], developed a force sensing system in which strain gauges were mounted on the structure and integrated to a tool holder, to monitor three cutting forces during the milling process. In other studies, a strain gauge-based torque measurement systems, called a smart tool holder, have been designed and developed. The developed rotary dynamometer systemshave shown high accuracy and resolution in measuring the cutting forces [1, 21, 22]. According to the number of capacitive sensors or strain gauges used in the measurement system, the developed solutions can measure two- or three-axis cutting force/torque. Yet thelimitation in this technique is that for measuring the cutting force/torque in each axis, one strain gauge sensor is required. For example, in the research conducted by Rizal *et al.* [6], three full-bridge Wheatstone circuits were constructed, and 24 strain gauges were used, which dramatically increases the complexity of the system while reducing the system's reliability [1].

In general, load cell and strain gauge are suitable solutions for industrial-level force measurement, as the most precise, reliable, and high-speed solutions for industrial applications. Load cells have become the preferred weighing sensor in many industrial settings due to the accuracy and speed with which they return data. To measure the amount of the applied force, strain gauge load cells are attached to industrial-scale platforms, vessel mounting legs, support beams, wire rope, cranes, and more. The force deforms the load cell to a small degree, converting the mechanical force into a proportional electrical signal that many types of electronics can measure. This information is very valuable for control systems for batching, process control, and material consumption [23]. The purpose of this research is to design and develop a high-precision self-sensing cutting force (SSCF) tool holder, for in-process metrology of cutting forces during ultra-precision machining processes, including single-point diamond turning (SPDT) process. Only a few solutions have been specifically designed and developed to be used in advanced manufacturing processes for in-process measurement of cutting forces. The proposed system contributes to the development of an integrated tool holder system, capable of measuring the cutting force during SPDT process.

2 DESIGN OF THE SYSTEM

In high-precision SPDT process, the cutting force has a small amount, around 1 N. The proposed system is designed to measure the applied force, in a range between 0 and 10 N, as well as measuring the applied torque in a range between 0 and 100 Nm, with high sampling speed, precision, and, resolution 0.1 N. In this study, a standard commercial toolholder, usually used in the standard SPDT platform, is re-engineered to create a deformable beam and to provide the mechanism a SSCF system. In the design of the system, two T-rosette strain gauges are used and fixed to the force sensing toolholder's surface, to distinguish the

deformation of the beams, and subsequently determine the cutting force based on the applied force and the resistance variation.

2.1 Theoretical analysis

In the designed system, the variation of the resistances of the applied strain-gauges should bemeasured so that the force, applied to the mechanism, can be calculated. For this purpose, theworking principles of the cantilever beam have been adopted to be used for analyzing the designed SSCF tool holder. The cantilever is a beam in which one side of the beam is fixed to a rigid structure and the other side is free. In case a load is applied to the free side of the beam, a deflection occurs, as illustrated in Fig. 1. In Fig. 1, when an external force is applied to point B, the stress and strain are the measurable parameters. Stress is defined asthe internal resisting forces of the object, and strain is defined as the occurrence of displacement and deformation. In this condition, for calculating the tension at point B, the following eqn (1) can be used:

$$\sigma = \frac{MC}{I} \tag{1}$$

where, M is the resulting bending moment, I is the moment of inertia of the cross-sectional area, and C is the distance from the neutral line to the point of interest. Also, the moment of inertia can be calculated using the eqn (2):

$$I = \frac{bh^3}{12} \tag{2}$$

where b is the width of the beam and h is the thickness of the beam. By considering eqns (1) and (2), where c becomes $\frac{h}{2}$, the following equation can be drawn for maximum allowable stress:

$$\sigma_{max} = \frac{6M}{bh^2} \tag{3}$$

where σ_{max} is the maximum tension on the surface of the beam and M is subjected to a bending moment. By using the Hook's law eqn (4), the deformation of the beam can be measured as follows:

$$\varepsilon = E\sigma \tag{4}$$

where ε is the maximum tension of the beam and E is the modulus of elastic of the material. By using eqns (3) and (4), the surface deformation of the beam, when subjected to bending can be calculated as follows:

$$\varepsilon = E\frac{6M}{bh^2} \tag{5}$$

2.2 Dynamic properties of the sensor

The frequency of vibration of the machine tool in which the self-sensor cutting force will be mounted on for cutting force measurement need to agree with natural frequency of the

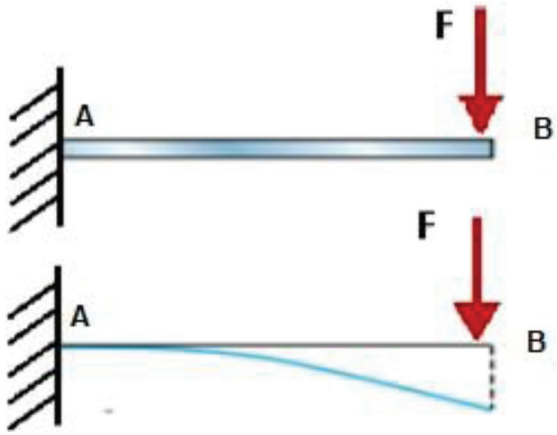

Figure 1: Cantilever beam before and after deflection.

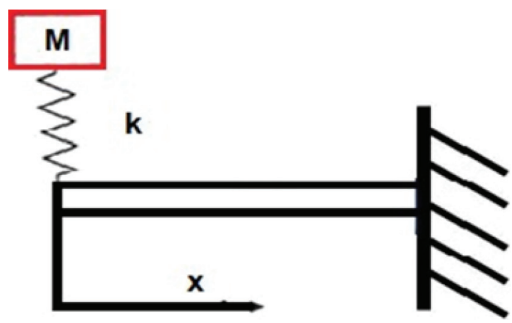

Figure 2: Structural diagram of the designed SSCF tool holder.

proposed system. This system can be considered as a dynamometer, as it can measure the applied force. Figure 2 illustrates the dynamic diagram of the designed SSCF tool holder mechanism. According to the literature [20], the natural frequency of a typical dynamometer should be as high as possible. The frequency of the vibration of the machine tool is similar to the spindle speed of the machine tool. Therefore, the SSCF tool holder should have natural frequency at least four times higher than vibration frequency of the machine tool [1, 16, 24–26]. The machine tool's vibration frequency can be calculated using the following equation:

$$f_m = \frac{\frac{n}{60} rev}{s} \tag{6}$$

where M = mass, K = stiffness, and X = length.

If the maximum spindle speed of the machine for the experiment is 3,000 rpm, then frequencyof the machine tool (Fm) is 50 Hz. Therefore, the natural frequency of the tool holder sensor should be as follows:

$$f_n \geq 4 \times \frac{\frac{n}{60} rev}{s} \tag{7}$$

$$f_n = \frac{1}{2\lambda}\sqrt{\frac{K}{M_t}} \tag{8}$$

$$K = \frac{3EI}{L^3} \tag{9}$$

$$M = pbdl \tag{10}$$

where *Fm* is the frequency of machine tool, *n* is the spindle speed (rpm), *Fn* is the natural frequencyof the tool holder, *K* is the stiffness, *M* is the total mass of the tool holder and strain gauges, *b* is the breadth, *d* is the width, and *l* is the length. From the design, I = 5942.125, E = 120 GPa, density (ρ) of the tool holder material (titanium) = 4,420 kg/m^3, area (A0) of the tool holderdesigned (b × d × L) = 1,350 mm^2. Therefore, to fulfil the requirement as stated above in eqn (1), if the frequency of the machine tool is 50 Hz, and the computed natural frequency of the tool holder is 807.5 Hz based on the relations in eqns (1)–(4), hence $Fn \geq 4\ Fm$.

2.3 Design and Development

In the design of the proposed system, a full-bridge Wheatstone bridge configuration is used. It is common to link one or more strain gauges aligned to respond to the maximum

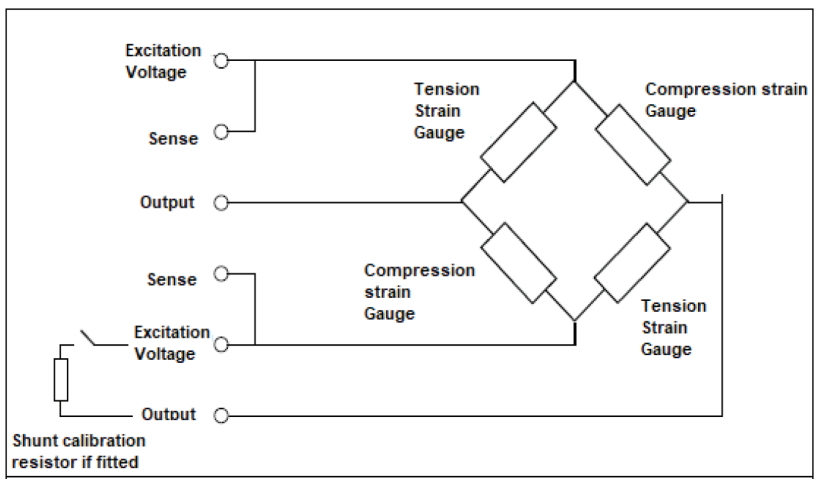

Figure 3: Structural diagram of the designed SSCF tool holder.

compressive strain and another set aligned to the maximum tensile strain to optimize the response of the load cell. This has the added benefit of minimizing the effects of environmental changes such as temperature, which work on all gauges equally, when linked electrically in a Wheatstone bridge configuration, as illustrated in Fig. 3. By evaluating the differential voltage across the bridge, the resistance change is observed. When excited by an input voltage, the voltage output from the bridge is connected linearly to the resistance change of the strain gauges and is therefore a function of the force applied to the element.

Mathematically, this is the product of the strain and the excitation voltage. The rated output ofa load cell may be standardized to a nominal level, usually 2 mV/V (i.e. 2 millivolts output per volt applied), but this may range from 1 to 4 mV/V. In the proposed system, metal foilstrain gauges are used, which are resistors with a nominal (unstrained) resistance of 350 ohms. In the structure of the metal foil strain gauge, two independent strain gauges with perpendicular grids on a single carrier have been used. By using this combination and attaching the strain gauges to the SSCF tool holder, measurement of the applied force is possible. Figure 4 presents the circuit design of the proposed system using metal foil strain gauges in full-bridge connections.

The fundamental formula for the resistance of a wire with uniform cross section, A, and resistivity, ρ, can be expressed as follows in eqn (11):

$$R = \rho \frac{L}{A} \tag{11}$$

where R is the resistance of the wire, ρ is the resistivity of the wire, L is the length of the wire, and A represents the cross section of the wire. The resistance changes per unit resistance ($\Delta R/R$) is as follows:

$$\frac{dR}{R} = \frac{d\rho}{\rho} + \left(1 + 2\nu\right)\varepsilon \tag{12}$$

where ε is the strain experienced in the material and ν is the position ratio, which serves as the ratio of lateral strain to axial strain on the material. In addition, one of the fundamental parameters of strain gauge is the gauge factor (GF). It is the measure of sensitivity of the sensor, or its resistance change per unit applied strain, as presented following:

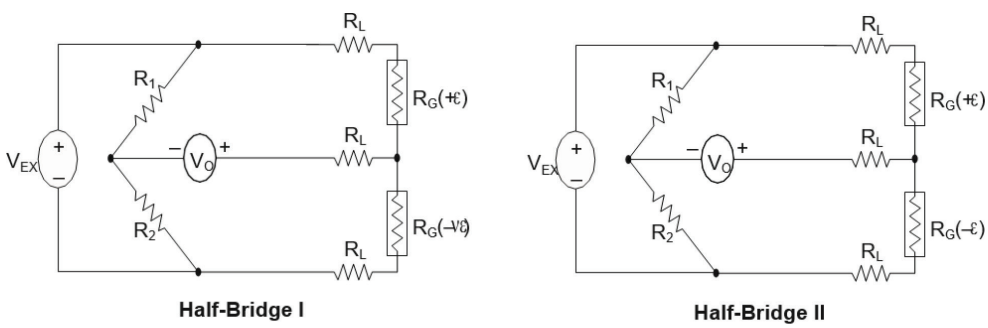

Figure 4: Half-bridge setup.

$$GF = 1 + 2\nu + \frac{\frac{d\rho}{\rho}}{s} \tag{13}$$

where GF is connotation for the gauge factor. The above expression of gauge factor includes effects from two aspects. The right term in eqn (8), represents the Poisson effect, which is the tendency in an elastic material to contract laterally in response to axial stretching. The left term in eqn (8), represents the contribution due to changes in resistivity of the material in response to the applied strain. In the absence of a direct resistivity change, the maximum and minimum values expected for the gauge factor can be presented as follows:

$$1 << GF << 2 \tag{14}$$

Typically, gauge factor is the ratio of fractional change in electrical resistance of a wire to the fraction in length. Therefore, a high value of gauge factor is better for strain gauge because it shows a high sensitivity to resistance of a wire and increases the output signal of the sensor. The gauge factor used in this study as supplied by manufacturer is 1.9. Figure 4 shows strain configuration for the chosen sensor, which is a half-bridge. This provides us with a linear strain output function. The half-bridge was chosen over a quarter-bridge in the intended system because of self-compensated strain gauges. This was made possible using two gauges that were well-matched to develop temperature compensation.

The full-bridge arrangement would have been a better alternative to the half-bridge arrangement shown in Fig. 4 in terms of device sensitivity, but because the elastic beam used was not very wide (0.0135 m), it would not have been practical to install and wire two gauges on the same sideof the beam. Hence, the half-bridge arrangement as preferred and chosen. In Fig. 4, for measuring the applied force, the strain of each circuit should be measured. By using the measured value, as well as the variation in the measured value, the strain changes in the applied strain gauge system can be measured. The following equations can be used for measuring the strain of the mechanism and its changes can be measured using the following eqns (15) and (16):

$$strain(\varepsilon) = \frac{-4\nu_f}{GF\left[(1+\nu) - 2V_f(\nu - 1)\right]} \times \left(1 + \frac{R_L}{R_G}\right) \tag{15}$$

$$strain(\varepsilon) = \frac{-2\nu_f}{GF} \times \left(1 + \frac{R_L}{R_G}\right) \tag{16}$$

where R_L = lead resistance, R_G = nominal gauge resistance, R_1 and R_2 = half-bridgecompletion resistors, $Vext$ = excitation voltage, Va = signal voltage, $R_G(+\varepsilon)$ = tensile strain, and $R_G(-\varepsilon)$ = compression strain.

After the design and development of the SSCF tool holder, it should be connected to a circuitfor measuring the resistance of the strain gauges. Subsequently, the output signals of the strain gauges should be captured, amplified, and measured so that the applied force can be calculated. Figure 5 illustrates the schematic design of the developed SSCF tool holder. As illustrated in Fig. 5, two T-rosettes were attached to the design; this represents four strain gauges on the cantilever beam.

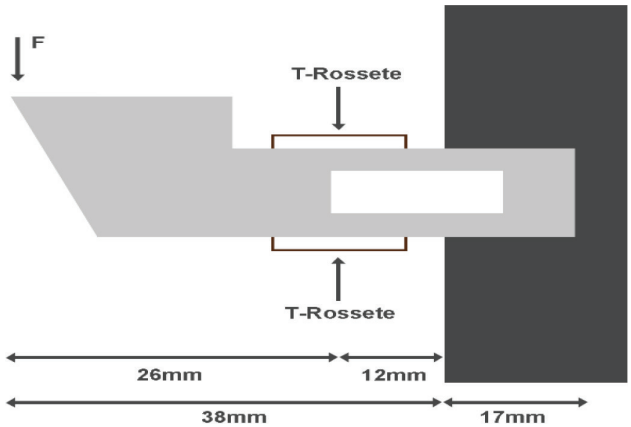

Figure 5: Schematic design.

The output signals are low-voltage analog signals with small changes. Therefore, the output pins of the T-rosettes should get connected to an amplifier to amplify the captured analog signal. Then, the amplified analog signal should be transferred to a microcontroller to distinguish the changes in the level of the voltage caused by the strain and then to calculate the applied force based on the measured resistance. Figure 6 presents the schematic of the designed system. In the designed system, an Arduino Micro development board with ATmega32U4 microcontroller and a HX711 load cell amplifier module has been used. The Arduino Micro is an ATmega32u4-based microcontroller module, with 20 digital input/output pins, a 16-MHz crystal oscillator. HX711 load cell amplifier is a high-precision 24-bit analog to digital converter designed for weigh scales and industrial control applications to interface directly with a bridge sensor.

During the SPDT process, a cutting force around 1 N is applied to the diamond tooltip. Therefore, the designed system experiences a small change in the resistance of the strain gauges, which can be captured in shape small changes in the output voltage of the system. In the HX711 amplifier, the input multiplexer selects the differential input between channel A or B. When a 5 V supply is connected to the supply pin of the amplifier, channel A can be used with a gain of 64 or 128, corresponding to a full-scale differential input voltage of ±20 mV or ±40 mV. Channel B has a constant gain of 32. Figure 7 presents the detailed circuit design of the system. A0–A5, A6–A11 analog inputs: (on digital pins 4, 6, 8, 9, 10, and 12). The micro has a total of 12 analog inputs, pins from A0 to A5 are numbered directly on the pins and pins 4, 6, 8, 9, 10, and 12 are shared on digital pins 4, 6, 8, 9, 10, and 12, respectively, on the other pins that you can access in code using the constants from A6 to A11. All of which can be used as digital I/O as well. Each analog input provides a resolution of 10 bits (i.e. 1,024 different values). The authors used pins A5, A4, ground, and 5 V for this research work. After the development of the system, the Arduino IDE software has been used to program the microcontroller, as well as calibration of the developed SSCF sensor.

2.4 Calibration of the sensor

2.4.1 Mechanical calibration

Based on this design, as stated previously that the maximum deflection of the designed tool holder can have $\delta max = 3.71 \times 10^{-5}$ mm. However, it is advisable to position the strain gauge

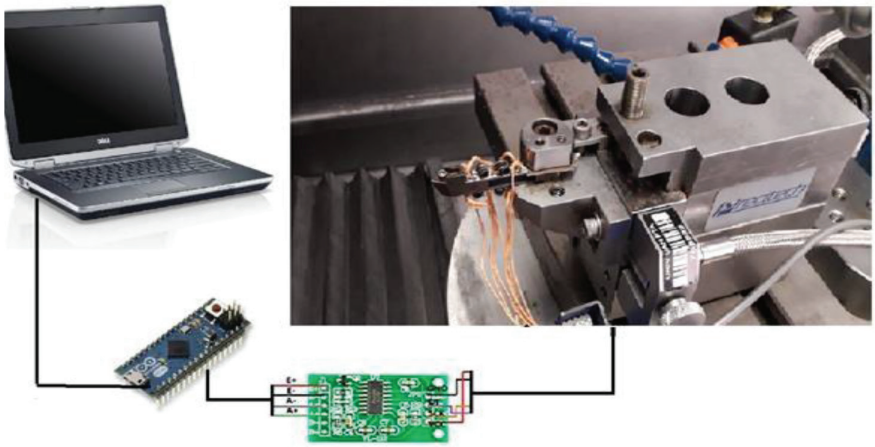

Figure 6: Schematic diagram of self-force sensor tool holder.

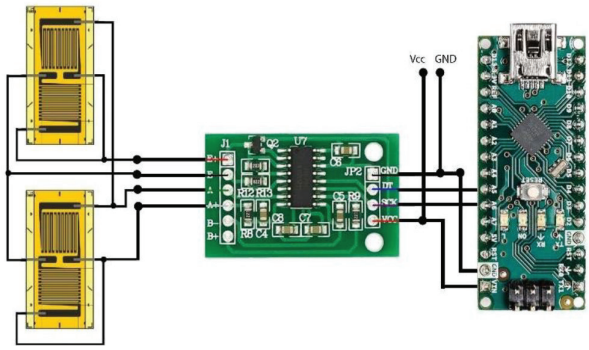

Figure 7: The detailed circuit design.

at the region where maximum stress is observed on the material because the plastic deformation activities due to loading (stress) can be sensed at this point. Next, the author discusses the linear relationship for Arduino analog converter, which can be used to calibratethe load cell if other means cannot be dimmed. In most cases, calibration of measuring instruments can be attained by comparing measurement results to a measurement standard.

It has relatively known resistance and some normal possible uncertainty. Considering linearrelationship on how to calibrate load cell, when a load M is applied to the beam causing the resistance to change. M can also be determined using simple linear equation:

$$y = mx + b \tag{17}$$

$$m = \frac{(y - b)}{x} \tag{18}$$

where m represents the slope in Fig. 8.

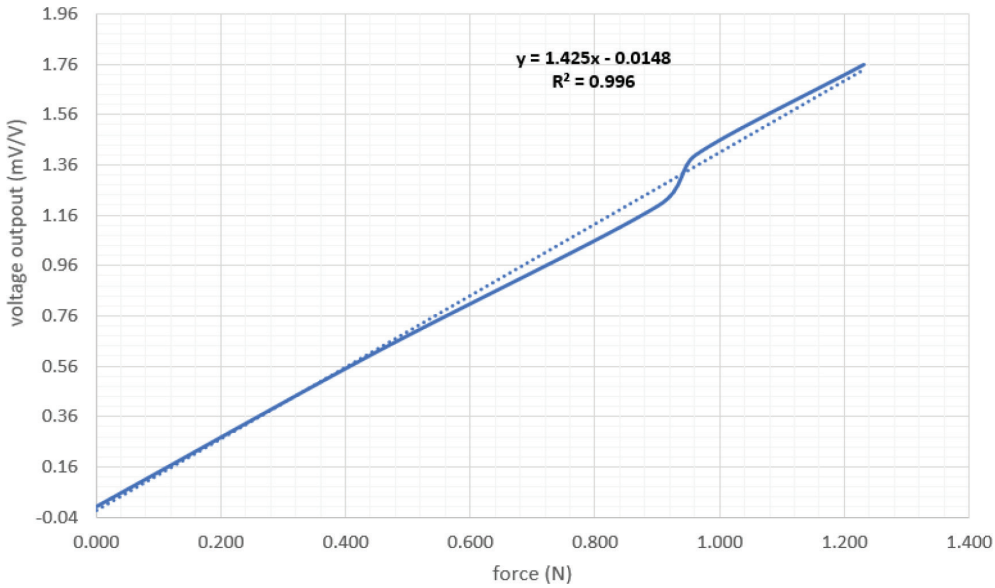

Figure 8: Sensor sensitivity curve for sensor calibration.

2.4.2 Voltage calibration

To calibrate the sensor, the followings are the T-rosette strain gauge parameters; excitation voltage of the load cell (T-rosette) is 4.5 V while resistance of the strain gauge (T-rosette) is 350 ohms. The gauge factor, which is also known as strain gauge sensitivity, is 1.95. Rated output of the gauge is 1 mV/V while the rated capacity we designed for in this study is 300 g equivalent to 2.94 N for maximum load. However, the maximum force expected during the machining is less than 2 N. Therefore, if rated output is 1 mV/V with known excitation of 4.5 V, the load cell output expected to be displayed for minimum of 1 g is 4.592 mV/N or 0.004592 V/N. This represents the sensitivity of the self-sensing cutting force tool holder (SSCFTH) designed. However, since data acquisition method is implemented in the research,a multiplier is required for our serial monitor during machining.

2.5 Experimental test

A series of experiments have been conducted, and the findings show that it is safe and realistic to accurately measure the cutting force in diamond turning processes. After careful review of literature, the following cutting parameters were adopted based on this material [13, 27–29]. Cutting speed from 500, 1,750, and 3,000 rpm, feed rates 5, 15, and 25 mm/min, and depth of cuts 5, 15, and 25 µm. The research experiments were carried out in such a way that an ultra-precision machine called Precitech Nanoform 250 ultra-grind lathe machine was usedto machine cylindrical Optical Aluminum alloy RSA 6061 where a SSCFTH was attached to the tool holder as seen in Fig. 5 to monitor the machining process. The cutting conditions used for cutting test are feed rates, cutting speed, and depth-of-cut.

Table 1: Weight results during static calibration.

Known weight (g)	Known weight (N)	Voltage output (mV/V)
0	0.000	0.00
44.6	0.438	0.61
92	0.903	1.22
98	0.961	1.41
125.5	1.231	1.76

3 RESULTS AND DISCUSSION

3.1 Calibration results

After the installation and mounting of the SSCFTH design, various known weights in Table 1 are used to calibrate the multiplier factor of the voltage output. Table 1 shows weights and the voltage outputs. During calibration, sensors are subjected to known quantities of physical measures, such as force, and the corresponding values of the output variable, which are recorded. The magnitude of this load is accurately known, as it is measured with a traceably calibrated against factory standard (Kistler force sensor) at the same time. Depending on the method, sensors are calibrated either across the entire measuring range or in a partial range: at a single point, continuously, or stepwise at several different points. The method adopted in this study is continuous although certain literature prefers step-by-step method. During continuous calibration, the load is continuously increased to a certain level within a defined capacity of the strain gauge and then reduced to zero within the same time. A best straight line passing through the origin is defined for the resultant characteristic. It should be noted that it is never always easy to get a perfect straight or exactly linear line. The gradient of this line corresponds to the sensitivity of the sensor within the calibrated measured range. A 99.6% accuracy is achieved for this study.

3.2 Machining results

In Figs. 9–12, the effects of cutting force are displayed at various machining parameters. Based on the experiments, the highest cutting force (see Fig. 11) was recorded at a high feed rate of 25 mm/min and depth-of-cut 25 µm, which bear witness to what is common in literature during diamond turning of advanced materials [30, 31]. We also noticed a decrease in cutting force that was compensated for by a high cutting speed and low feed rate as shown in Fig. 12 [32–34]. These two characteristics displayed shows the validity of SSCFTH designed. The two effects described above can be very useful to monitor power consumption and surface qualityof advance materials during diamond turning [35, 36].

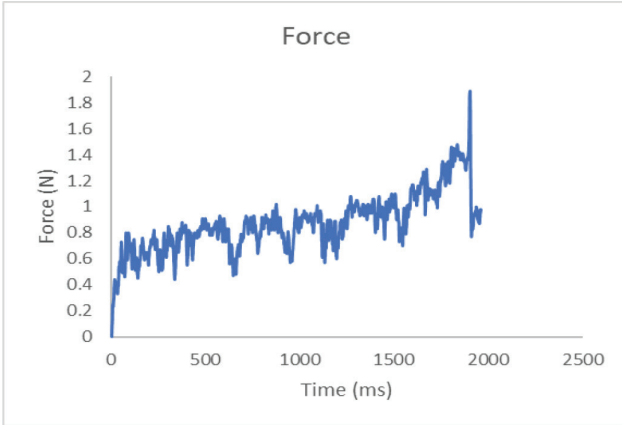

Figure 9: Cutting speed = 500 (rpm), feed rate = 5 (mm/min), depth-of-cut = 15 (μm), force average = 0.9 (N).

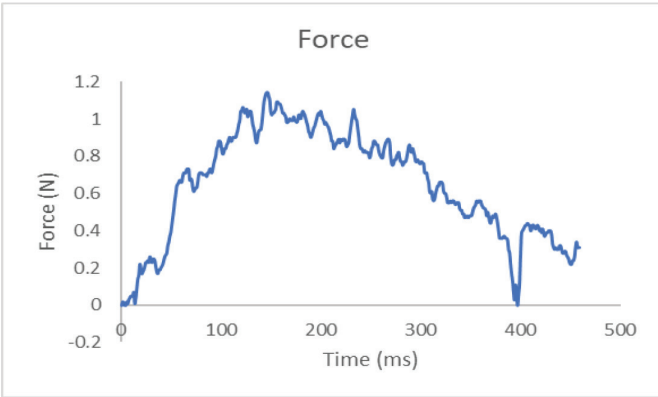

Figure 10: Cutting speed = 3,000 (rpm), feed rate = 25 (mm/min), depth-of-cut = 15 (μm), force average = 0.71 (N).

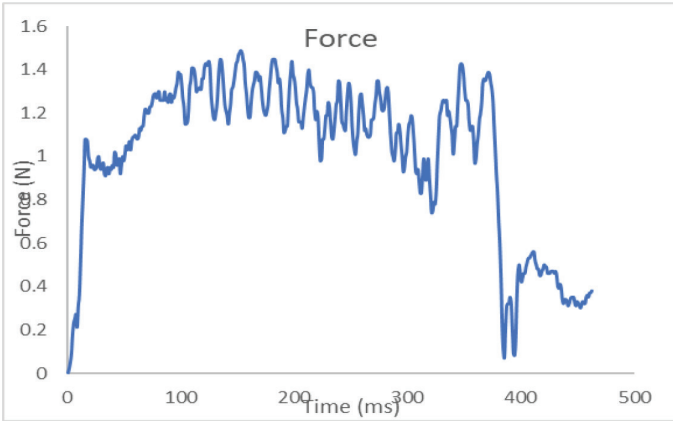

Figure 11: Cutting speed = 1,750 (rpm), feed rate = 25 (mm/min), depth-of-cut = 25 (μm), force average= 1.07 (N).

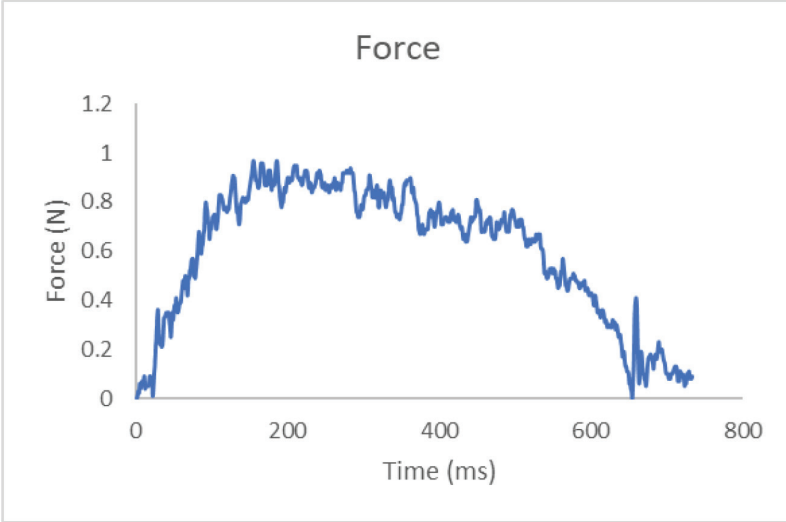

Figure 12: Cutting speed = 3,000 (rpm), feed rate = 15 (mm/min), depth-of-cut = 25 (μm), force average = 0.66 (N).

4 CONCLUSIONS

In this work, a tool holder based on strain gauge sensor for measuring cutting force during ultra-precision diamond turning was designed and developed, which can be used as a simple dynamometer. A standard cantilever beam tool holder was modified to make itself the force-sensing element, which has advantages of simple structure over industrial dynamometer and easy machining. A 2 T-rosette strain gauge sensors and other choice of electronics, such as data acquisition were integrated into the tool holder making it a whole system. The device is well-suited with various standard of cutting tools, thus providing a flexible and reconfigurable machining process. A few tests have been carried out to evaluate the performance of the SSCF tool holder developed.

Furthermore, the device has the benefits of simple construction and low cost, making it easyto manufacture and ideal for industrial use. The findings will be summed as follows:

- Static calibration tests have shown that the new system can assess cutting intensity up to3N with a high sensitivity of 4.592 mV/N or 0.004592 V/N and a calibration test variabilityof 99.6% has been achieved.
- The designed and developed SSCF tool holder showed a natural frequency of approximately 807.5 Hz of the tool holder spindle mechanism, which means that its dynamic range is appropriate for machining up to 3,000 rpm of spindle speed while usinga diamond tool.
- Diamond turning experiments have been carried out and the results have shown that the SSCF tool holder system is capable of measuring cutting force in a timely and reliable manner with three statistical indicators as follows: percentage error is 2.19, MAPE is 17.57%, and RMSE is 0.43 relative to the industrial table dynamometer.

ACKNOWLEDGEMENTS

The authors would like to thank the National Research Foundation (NRF/DAAD) of South Africa and the Research Development of Nelson Mandela University (NMU) for theirsupport of this research.

NOMENCLATURE

σ	Tension of the surface (N/m)	X	Length (m)
M	Bending moment (N.m)	b	Breadth (m)
C	Distance (m)	d	Width (m)
I	Moment of inertia (kg/m^2)	l	Length (m)
b	Width of the beam (m)	ρ	Density (kg/ m$^{3)}$
h	Thickness of the beam (m)	A	Area (m^2)
ε	Maximum tension of the beam (N/m)	R	Resistance (Ω)
E	Modulus of elasticity of the material (Gpa)	ρ	Resistivity (Ω.m)
fm	Frequency of the machine tool (Hz)	ε	Strain in the material
fn	Natural frequency of the tool holder (Hz)	v	Position ratio (ratio of lateral strain to axial strain)
n	Spindle speed (rpm)		
M	Total mass of the tool holder and strain gauge (kg)	GF	Connotation for the gauge factor
		V	Voltage (V)
K	Stiffness of the tool holder (N.m/rad)		

REFERENCES

[1] Mohanraj, T., Shankar, S., Rajasekar, R. & Uddin, M., Design, development, calibration, and testing of indigenously developed strain gauge based dynamometer for cuttingforce measurement in the milling process. *Journal of Mechanical Engineering and Sciences,* **14**, pp. 6594–6609, 2020. https://doi.org/10.15282/jmes.14.2.2020.05.0517

[2] Wang, J., Zuo, J., Shang, Z., Fan, X., Modeling of cutting force prediction in machininghigh-volume SiCp/Al composites. *Applied Mathematical Modelling,* **70**, pp. 1–17, 2019. https://doi.org/10.1016/j.apm.2019.01.015

[3] Sawangsri, W. & Cheng, K., An innovative approach to cutting force modelling in diamond turning and its correlation analysis with tool wear. *Proceedings of the Institution of Mechanical Engineers, Part B: Journal of Engineering Manufacture,* **230**, pp. 405–415, 2016.

[4] Uquillas, D. A. R. & Yeh, S.-S., Tool holder sensor design for measuring the cutting force in CNC turning machines. In *2015 IEEE International Conference on Advanced Intelligent Mechatronics (AIM)*, pp. 1218–1223, 2015.

[5] Ryabov, O., Kano, S., Sawada, H. & Herwan, J., Lathe machine as Industrie 4.0 Component (CPS). In *2019 IEEE 28th International Symposium on Industrial Electronics (ISIE)*, **2019**, pp. 1656–1660.

[6] Lyu, Y., Jamil, M., He, N., Gupta, M. K. & Pimenov, D. Y., Development and testing of a high-frequency dynamometer for high-speed milling process. *Machines*, **9**, p. 11, 2021. https://doi.org/10.3390/machines9010011

[7] Cus, F., Milfelner, M. & Balic, J., An intelligent system for monitoring and optimization of ball-end milling process. *Journal of Materials Processing Technology,* **175**, pp. 90–97, 2006. https://doi.org/10.1016/j.jmatprotec.2005.04.041

[8] Mohanraj, T., Shankar, S., Rajasekar, R., Sakthivel, N. R. & Pramanik, A., Tool condition monitoring techniques in milling process—a review. *Journal of Materials Research and Technology*, **9**, pp. 1032–1042, 2020. https://doi.org/10.1016/j.jmrt.2019.10.031

[9] Shankar, S., Mohanraj, T. & Rajasekar, R., Prediction of cutting tool wear during milling process using artificial intelligence techniques. *International Journal of Computer Integrated Manufacturing*, **32**, pp. 174–182, 2019. https://doi.org/10.1080/0951192x.2018.1550681

[10] SK, T. & Shankarm S., Tool wear prediction in hard turning of EN8 steel using cutting force and surface roughness with artificial neural network. *Proceedings of the Institution of Mechanical Engineers, Part C: Journal of Mechanical Engineering Science*, **234**, pp. 329–342, 2020.

[11] Cheng, K., Niu, Z. C., Wang, R. C., Rakowski, R. & Bateman, R., Smart cutting tools and smart machining: development approaches, and their implementation and application perspectives. *Chinese Journal of Mechanical Engineering*, **30**, pp. 1162–1176, 2017. https://doi.org/10.1007/s10033-017-0183-4

[12] Xiao, C., Ding, H., Cheng, K. & Chen, S., Design of an innovative smart turning tool with application to real-time cutting force measurement. *Proceedings of the Institution of Mechanical Engineers, Part B: Journal of Engineering Manufacture*, **229**, pp. 563–568, 2015.

[13] Otieno, T. & Abou-El-Hossein, K., Cutting forces and acoustic emission in the diamond turning of rapidly-solidified aluminium. *Insight-Non-Destructive Testing and Condition Monitoring,* **60**, pp. 11–18, 2018. https://doi.org/10.1784/insi.2018.60.1.11

[14] Byrne, G. & O'Donnell, G., An integrated force sensor solution for process monitoring of drilling operations. *CIRP annals,* **56**, pp. 89–92, 2007. https://doi.org/10.1016/j.cirp.2007.05.023

[15] Bretz, A., Abele, E. & Weigold, M., Measuring the bore straightness during reaming with sensoric tools. *Production Engineering,* **14**, pp. 535–544, 2020. https://doi.org/10.1007/s11740-020-00977-6

[16] Totis, G., Wirtz, G., Sortino, M., Veselovac, D., Kuljanic, E. & Klocke, F., Development of a dynamometer for measuring individual cutting edge forces in face milling. *Mechanical Systems and Signal Processing,* **24**, pp. 1844–1857, 2010. https://doi.org/10.1016/j.ymssp.2010.02.010

[17] Ma, L., Melkote, S. N., Morehouse, J. B., Castle, J. B., Fonda, J. W. & Johnson, M. A., Thin-film PVDF sensor-based monitoring of cutting forces in peripheral end milling. *Journal of Dynamic Systems, Measurement, and Control,* **134**, 2012.

[18] Ma, L., Melkote, S. N. & Castle, J. B., PVDF sensor-based monitoring of milling torque. *The International Journal of Advanced Manufacturing Technology,* **70**, pp. 1603–1614, 2014. https://doi.org/10.1007/s00170-013-5410-2

[19] Albrecht, A., Park, S. S., Altintas, Y. & Pritschow, G., High frequency bandwidth cutting force measurement in milling using capacitance displacement sensors. *International Journal of Machine Tools and Manufacture,* **45**, pp. 993–1008, 2005. https://doi.org/10.1016/j.ijmachtools.2004.11.028

[20] Guo, K., Zhao, Y., Zan, Z. & Sun, J., Development and testing of a wireless rotating triaxial vibration measuring tool holder system for milling process. *Measurement,* p. 108034, 2020.

[21] Suprock, C. A. & Nichols, J. S., A low cost wireless high bandwidth transmitter for sensor-integrated metal cutting tools and process monitoring. *International Journal of Mechatronics and Manufacturing Systems,* **2**, pp. 441–454, 2009. https://doi.org/10.1504/ijmms.2009.027128

[22] Nichols, J. S., Design and application of a wireless torque sensor for CNC milling. 2009.

[23] Silva, A. L., Varanis, M., Mereles, A. G., Oliveira, C. & Balthazar, J. M., A study of strain and deformation measurement using the Arduino microcontroller and strain gauges devices. *Revista Brasileira de Ensino de Física,* **41**, 2018.

[24] Shaw, M., *Metal cutting principles*. Clarendon. ed: Oxford, 1984.

[25] Öztürk, E. & Yıldızlı, K., Measured cutting forces in the turning of prismatic parts at different spindle speeds and side cutting edge angles. *Arabian Journal for Science and Engineering,* **43**, pp. 4635–4647, 2018. https://doi.org/10.1007/s13369-017-3002-4

[26] Silva, A. L., Varanis, M., Mereles, A. G., Oliveira, C. & Balthazar, J. M., A study of strain and deformation measurement using the Arduino microcontroller and strain gauges devices. *Revista Brasileira de Ensino de Física,* **41**, 2019.

[27] Cheng, Y.-C., Hsu, W.-Y., Abou-El-Hossein, K., Olufayo, O. & Otieno, T., Investigation of diamond turning: of rapidly solidified aluminum alloys. *Current Developments in Lens Design and Optical Engineering XV*, p. 919214, 2014.

[28] Cheng, Y.-C., Hsu, W.-Y., Kuo, C.-H., Abou-El-Hossein, K. & Otieno, T., Investigation of rapidly solidified aluminum by using diamond turning and a magnetorheological finishing process. in *Optical Manufacturing and Testing XI*, p. 957519, 2015.

[29] Otieno, T., *The machinability of rapidly solidified aluminium alloy for optical mould inserts*. Nelson Mandela University, 2018.

[30] Shalaby, M., El Hakim, M., Veldhuis, S. & Dosbaeva, G., An investigation into the behavior of the cutting forces in precision turning. *The International Journal of Advanced Manufacturing Technology,* **90**, pp. 1605–1615, 2017. https://doi.org/10.1007/s00170-016-9465-8

[31] Qian, L. & Hossan, M. R., Effect on cutting force in turning hardened tool steels with cubic boron nitride inserts. *Journal of Materials Processing Technology,* **191**, pp. 274–278, 2007. https://doi.org/10.1016/j.jmatprotec.2007.03.022

[32] Liman, M. M. & Abou-El-Hossein, K., Modeling and multiresponse optimization of cutting parameters in SPDT of a rigid contact lens polymer using RSM and desirability function. *The International Journal of Advanced Manufacturing Technology,* **102**, pp. 1443–1465, 2019. https://doi.org/10.1007/s00170-018-3169-1

[33] Singh, K., Vaishya, R. O., Singh, H., Mishra, V. & Ramagopal, S., Investigation of tool life & surface roughness during single point diamond turning of silicon. *International Journal of Scientific Research,* **2**, pp. 265–267, 2013. https://doi.org/10.15373/22778179/june2013/84

[34] Luo, X., Cheng, K., Guo, X. & Holt, R., An investigation on the mechanics of nanometric cutting and the development of its test-bed. *International Journal of Production Research,* **41**, pp. 1449–1465, 2003. https://doi.org/10.1080/0020754031000069607

[35] Valera, H. Y. & Bhavsar, S. N., Experimental investigation of surface roughness and power consumption in turning operation of EN 31 alloy steel. *Procedia Technology,* **14**, pp. 528–534, 2014.

[36] Abdulkadir, L. N., Abou-El-Hossein, K., Jumare, A. I., Odedeyi, P. B., Liman, M. M. & Olaniyan, T. A., Ultra-precision diamond turning of optical silicon—a review. *The International Journal of Advanced Manufacturing Technology,* **96**, pp. 173–208, 2018. https://doi.org/10.1007/s00170-017-1529-x